Mathematical Geosciences (2025) 57:577–599
https://doi.org/10.1007/s11004-024-10174-1

Drill Pattern Optimisation for Large Complex Blasts to Improve Fragmentation and Dig Efficiency

Ozan Perincek[1,2] · Ryan Loxton[2] · Sarang Kulkarni[2] · Daniel Arthur[1,3]

Received: 16 October 2023 / Accepted: 15 December 2024 / Published online: 28 January 2025

Abstract

At large-scale open-pit metallic mines, drill-and-blast designs can reach over 1,000 drill holes per blast. A critical input to the design of a blast is the location of sensitive zones where ground vibration, air overpressure or flyrock needs to be constrained. The other critical input is the hardness profile of the ground. Often, the hardness across such large blasts varies significantly from soft to extra hard. Traditional approaches for pattern design use constant distance (burden and spacing) between the production drill holes and vary the explosive product strength and amount in each hole to account for variation in hardness and to adhere to blast constraints. Although this approach is operationally easier to execute, it is challenging to meet fragmentation and diggability objectives. To better address these objectives, this work provides a nonlinear mathematical model for optimising drill hole locations in conjunction with explosive amounts. The model optimises the design using a three-stage methodology. In the first stage, a novel heuristic method is used to perform local optimisation to determine the number of holes. In the second stage, the precise hole locations are determined, and in the third stage the energy intensity in each hole is optimised. In a study of 10 blasts from a Pilbara iron ore mine, for the dig efficiency objective, results indicate that variable designs achieve ∼2% better dig efficiency, with ∼11% fewer holes. For the fragmentation objective, variable designs achieve ∼9% better adherence to the target mean particle size, with ∼5% less standard deviation and ∼13% fewer holes.

Keywords Nonlinear modelling · Heuristic methods · Drill and blast · Mining

✉ Ozan Perincek
ozan.perincek@riotinto.com

1 Rio Tinto, Perth, Western Australia, Australia

2 Curtin University, Perth, Western Australia, Australia

3 Caltech, Pasadena, California, USA

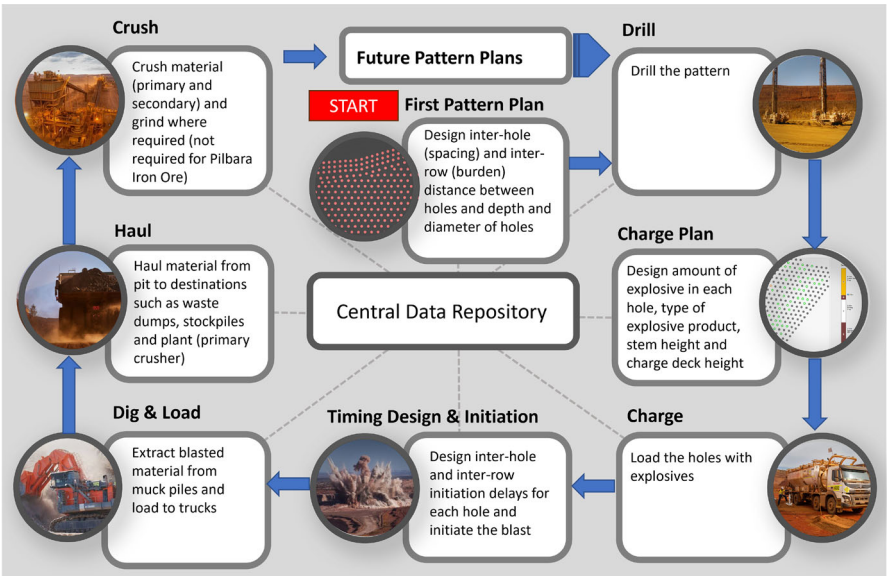

Fig. 1 Ore extraction process starts at the drill design and ends at the crushing of material (Haugg et al. 2023)

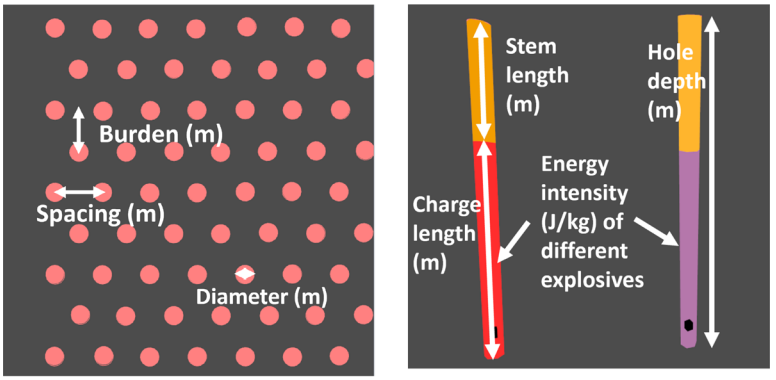

(a) Top down view of pattern (b) Side profile view of two holes

Fig. 2 Drill and Blast Decision Variables

1 Introduction

In surface mining operations, drilling and blasting (D&B) is one of the first steps in the ore extraction process (Fig. 1), and decisions made during D&B design have significant downstream impacts. This paper builds a mathematical model to optimise these D&B decision variables (Fig. 2) to meet dig efficiency objectives and to deliver material within the required particle size range to the crusher.

The model aims to cater to the complexity of varying ground hardness by spatially customising D&B designs. Traditional methods consider the burden (distance between

rows of holes) and spacing (distance between holes in the same row) as constant across the blast pattern (Aryafar et al. 2020; Bakhtavar et al. 2021, 2017; Cunningham 2005; Ouchterlony and Sanchidrián 2019; Salmi and Sellers 2021; Singh et al. 2016). In this paper, the burden and spacing are allowed to vary across the blast to account for variation in hardness and distance from sensitive sites. The hardness profile here is defined by categorical classification of the ground using measurement-while-drilling (MWD) data. The method for estimating hardness is summarised in Sect. 2 and detailed in Haugg et al. (2023). Our model also involves optimising other decision variables, including hole diameter, depth, and the energy intensity required for each hole in the blast (see Fig. 2).

Executing such variable designs in traditional drilling and charging operations has been challenging due to the difficulty in determining precise geological properties and the operational complexity of manual drill navigation. However, automation and digital data now make this a more viable proposition. Enablers include the following:

1. Objective and high-resolution (burden $\times$ spacing resolution) prediction of ground hardness using MWD data from autonomous drills (Haugg et al. 2023).
2. Ability to execute complex blast designs using semi-automated trucks, known as mobile processing units (MPUs), that mix explosive ingredients in the field to produce the required product strength, identify hole ID and precisely deliver the corresponding design.
3. Access to large operational datasets from mine sites to model the impact of D&B decision variables on downstream processes.
4. Ability to precisely vary the detonation delays between holes using electronic detonators (this is not a recent advancement, but it is an enabler).

D&B optimisation has been widely studied with different objectives. Recent work by Bakhtavar et al. (2021) used mixed-integer programming (MIP) to minimise total mining costs associated with blasting. Total costs include downstream costs such as additional loading, hauling, crushing and secondary blasting (the need to blast large rocks for a second time) and undesirable impacts such as ground vibration, flyrock, air overpressure and dust. Later work addressing these adverse effects and improving outcomes used genetic programming (Hosseini et al. 2022) and included qualitative and quantitative analysis (Bakhtavar et al. 2022) to optimise blasts.

Other research focused on multi-attribute decision-making (MADM) to select the most suitable D&B parameters from a list of previously used values by linking these inputs to the outcomes of previous blasts (Aryafar et al. 2020; Bakhtavar et al. 2017; Yari et al. 2015; Mokhtari and Monjezi 2015). Khoshrou et al. (2010) also used regression analysis to calculate the optimal burden for a given set of blasting parameters such as hole diameter. There have also been attempts to use machine learning for predicting and optimising D&B designs (Esmaeili et al. 2015; Enayatollahi et al. 2014; Monjezi et al. 2010; Monjezi and Bahrami 2010b; Jia et al. 2022; Fang et al. 2021; Hasanipanah et al. 2018; Ebrahimi et al. 2016; Zhou et al. 2021). Zhou et al. (2024) present a comprehensive review of these approaches.

The above-mentioned studies consider a constant burden and spacing across the blast. The use of constant burden and spacing ignores the effect of variation in geological properties and the impact of constraints on hole positions. Our model allows

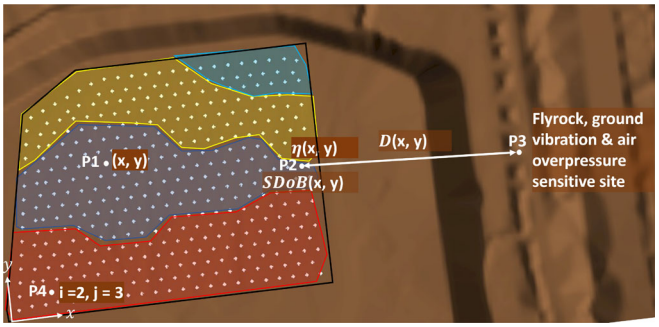

Fig. 3 Top-down view of a design illustrating hole positions (in white), a sensitive site and ground hardness. Red is soft, yellow is medium, light blue is hard and dark blue is extra hard

variation in burden and spacing while determining the optimal location of each hole in the blast.

Section 2 presents a mathematical model that requires high-precision geological properties across the blast as an input. The model is complex because the precise number of holes is unknown a priori, and the ground hardness is only known at discrete points (at the locations of previously drilled holes). Hardness needs to be interpolated at intermediate points using weighted averages, and the challenge is to determine the model inputs for a given hole without knowledge of the exact position. In addition, some functions, such as the maximum explosive energy that can be used in a hole for a given hardness, are discontinuous. To overcome these challenges, a novel approach is proposed in Sect. 3 that first determines approximate positions for each hole individually and then, using the ground characteristics for a small region around each hole, optimises for exact locations of holes and other decision variables simultaneously. The above process uses a nonlinear model to determine all of the required parameters of the design, and upon validation by a D&B designer, the design can be sent to an autonomous drill system for execution.

Section 4 compares outcomes from historical pattern designs from a Rio Tinto-operated mine in the Pilbara to simulated outcomes from the above-mentioned approach. The results show that both dig efficiency and fragmentation can be improved by estimating hardness at high resolution and by adjusting burden and spacing to account for this variance in hardness.

2 Problem Description

Consider a design scenario (or a blast pattern) as shown in Fig. 3. The black line shows the extent of the blast and the white dots indicate holes. Assume that the number of rows, $\{1, \ldots, I\}$, and the number of columns, $\{1, \ldots, J_i\}$, in each row $i \in \{1, \ldots, I\}$ are given. Later, in Sect. 3, we explain how these values can be calculated. Also, assume that there is a sensitive site at a fixed location that needs to be protected. The goal is to determine the exact locations of the holes and the energy intensity in each hole to achieve the required objective (either fragmentation or dig efficiency).

The D&B design is constrained by four requirements:

1. Energy intensity: Limit the energy intensity of the explosive product in each hole to a specified value that depends on the ground hardness.
2. Ground vibration: Limit the peak particle velocity (PPV) to restrict ground vibration at the sensitive site.
3. Air overpressure: Limit the air overpressure (AOP) to protect fauna at the sensitive site.
4. Flyrock: Limit the flyrock at the sensitive site by controlling the scaled depth of burial (SDoB) through the stem length.

In the subsections to follow, we introduce the decisions and input parameters and describe the objectives and constraints in detail.

2.1 Decision Variables and Input Parameters

The following are the decision variables for a hole at row $i \in \{1, \ldots, I\}$ and column $j \in \{1, \ldots, J_i\}$: B_{ij} is burden, S_{ij} is spacing, ϕ_{ij} is diameter, d_{ij} is depth, sl_{ij} is stem length, Q_{ij} is mass of explosives, ρ_{ij} is density of explosive product, ε_{ij} is energy intensity of the explosive product and R_{ij} is weight strength of the explosive product relative to ammonia nitrate fuel. Although diameter, ϕ, is defined above as a local decision variable for each hole, it is actually a global decision variable shared by all holes. This is because it is operationally complex to frequently change the drill bit across the blast.

We require the global input parameter H, bench height, and the following input parameters for each hole at row $i \in \{1, \ldots, I\}$ and column $j \in \{1, \ldots, J_i\}$: η_{ij} is the hardness of the ground, E^0_{ij} is the energy concentration for maximum excavator efficiency (which is a function of hardness), D_{ij} is the distance to the sensitive site, $\varepsilon^{\max}_{ij}$ is the maximum allowed energy intensity (depending on the ground hardness), $d^{\min}_{ij}$ is the minimum hole depth required to achieve the desired bench height, and $SDoB_{ij}$ is the scaled depth of burial (which depends on the distance from the sensitive site and influences the stem length of the hole).

Ground Hardness

One of the key design inputs is the hardness profile of the ground, which is traditionally determined by mine geologists using different data sources. However, with advances in drilling technology, the hardness, η, can now be estimated automatically using MWD data. One method for predicting hardness, proposed by Haugg et al. (2023), involves three steps:

1. Train a supervised machine learning model with drill torque, weight on bit, rotation speed, and penetration rate as the features and density measurements from a downhole probe as the labels. This model provides a way of estimating the density given the MWD data.
2. Compare the density predictions from the machine learning model with the geologist's classifications to establish thresholds for mapping density to hardness. For example, establish a range of densities for soft, another range of densities for

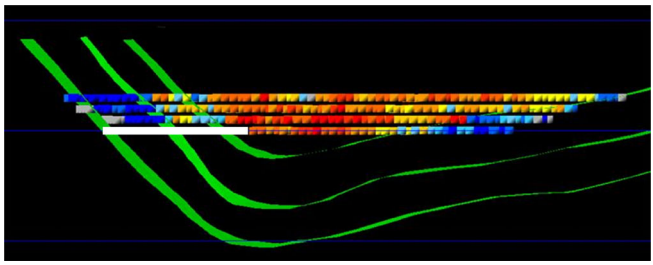

Fig. 4 Cross-sectional view of pit, showing planned drill area (in white) and previously drilled holes. Red is soft, yellow is medium, light blue is hard and dark blue is extra hard (Haugg et al. 2023)

medium, and so on. This enables the conversion of density prediction from MWD data to a hardness value.

3. Using the hardness estimates of previously drilled holes, project the hardness to the current mid-z value of a planned hole using the inverse-distance-squared model in (1).

The above method provides a fast and fit-for-purpose estimation of ground hardness and is further detailed in Perincek et al. (2024). For D&B optimisation, our model uses pre-specified data from steps 1 and 2. Step 3 can be substituted by any other method, including modelling anisotropies or an adaptive inverse distance weighting (Lu and Wong 2008).

Figure 4 shows the cross-sectional view of the pit with hardness predictions from previously drilled holes, shown by coloured squares. These are projected to x and y locations within the white zone in Fig. 4 to provide two-dimensional hardness zones, as shown in Fig. 3.

$$\eta(x, y) = \frac{\sum_{p=1}^{N} \omega_p \eta_p}{\sum_{p=1}^{N} \omega_p}, \tag{1}$$

where

$$\omega_p = \frac{1}{|x - x_p|^2 + |y - y_p|^2}, \tag{2}$$

where N is the number of drill holes from previous benches in the pit, η_p is discrete hardness values from the previous holes estimated by the MWD model, and x_p, y_p are the x and y coordinates of the previous holes.

Adjusted Burden and Spacing

Traditionally, the holes are located with constant burden, B (distance between rows), and spacing, S (distance between columns), for the entire blast pattern. However, in this paper, the burden and spacing are allowed to change across the blast. Hence, for any row $i \in \{1, \ldots, I\}$, an adjusted burden $\hat{B}_i$, and for any column $j \in \{1, \ldots, J_i\}$, an adjusted spacing $\hat{S}_{ij}$ are defined as shown in Fig. 5 and calculated by Eqs. (3) and

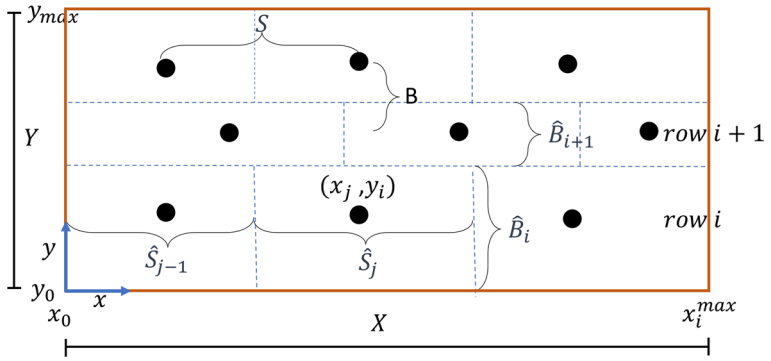

Fig. 5 Re-definition of conventional burden and spacing (top-down view)

(4).

$$\hat{S}_{ij} = \begin{cases} \dfrac{x_{i,j+1} + x_{i,j}}{2} - x_{i0}, & \text{if } j = 1, \\ \dfrac{x_{i,j+1} - x_{i,j-1}}{2}, & \text{if } 1 < j < J_i, \\ x_i^{\max} - \dfrac{x_{i,j} + x_{i,j-1}}{2}, & \text{if } j = J_i, \end{cases} \tag{3}$$

$$\hat{B}_i = \begin{cases} \dfrac{y_{i+1} + y_i}{2} - y_0, & \text{if } i = 1, \\ \dfrac{y_{i+1} - y_{i-1}}{2}, & \text{if } 1 < i < I, \\ y_{\max} - \dfrac{y_i + y_{i-1}}{2}, & \text{if } i = I, \end{cases} \tag{4}$$

where $\hat{B}_i$ is the adjusted burden for holes in row i (m), $\hat{S}_{ij}$ is the adjusted spacing for the hole at row i column j (m), x_{ij} is the x-axis value of the hole at row i column j (m), $x_{i0}, x_i^{\max}$ are the min and max x-axis values defining blast extents (m), y_i is the y-axis value of row i (m) and y_0, $y_{\max}$ are the min and max y-axis values defining blast extents (m).

As discussed in the introduction, we use two different objectives, dig efficiency and fragmentation. Next, we present the motivation and equations to model these objectives.

2.2 Dig Efficiency Objective

Segarra et al. (2010) created a model (Eq. (5) below) for expressing excavator efficiency, f_B, as a function of blast energy. Equation (5) states that low energy concentrations produce tight muck piles with high cohesion, which are difficult to dig. As blast energy increases, material flows more easily, and the muck pile becomes flatter. At E^0, the dig efficiency peaks, and further increases in blasting energy cause a decrease in dig efficiency. This is because muck piles become very flat with a low

angle of repose, requiring multiple passes to fill the dig unit bucket. Equation (5) is the motivation for the dig efficiency objective shown in Eq. (8).

$$f_B = \frac{\sigma^2}{(E - E^0)^2 + \sigma^2}, \tag{5}$$

where σ is the efficiency scale factor, E^0 is the explosive energy concentration at which excavator efficiency is maximised (J/m^3) and E is the explosive energy powder factor (J/m^3) as given by Eq. 6.

$$E = \frac{Q\varepsilon}{HBS}, \tag{6}$$

where

$$Q = \pi \left(\frac{\phi}{2}\right)^2 \rho(d - sl), \tag{7}$$

where Q is the mass of the explosive (kg), ϕ is the diameter of the holes (m), ρ is the density of the explosive product (kg/m^3), d is the depth of the hole (m), sl is the stemming length (m), ε is the energy intensity of the explosive product (J/kg), H is the blast bench height (m), B is the conventional burden (m) and S is the conventional spacing (m).

The value of E^0 depends on the hardness of the ground, and the hardness depends on the location of the hole. Salmi and Sellers (2021) outline several different blastability and hardness indices where, depending on the material type, an appropriate powder factor can be used. For example, Salmi and Sellers (2021) recommend a powder factor of $1.25 kg/m^3$ for "sandy shale". The explosive energy powder factor, E^0, is the product of the recommended powder factor for the hardness type and the energy intensity of the explosive product.

The first objective function, minimisation of deviation from the optimal energy concentration, $(E - E^0)^2$, and therefore the maximisation of dig efficiency, is

$$\min Z = \sum_{i=1}^{I} \sum_{j=1}^{J_i} \left[\frac{Q_{ij}\varepsilon_{ij}}{H\hat{B}_i\hat{S}_{ij}} - E^0_{ij} \right]^2. \tag{8}$$

Note that there are a discrete number of explosive products available at each site, and hence values of ε_{ij} and ρ_{ij} are linked and belong to a discrete set. Additionally, E^0 is a discontinuous function because the optimal energy concentration is only provided for a discrete number of hardness types. These challenges are addressed in Sect. 3.

2.3 Fragmentation Objective

Many different fragmentation formulas have been proposed in the literature. The Kuz-Ram formula was established based on the Kuznetsov and Rosin–Rammler equations

(Cunningham 1987, 2005). Ouchterlony (2005) developed the Swebrec function to improve prediction of fines. Researchers at the Julius Kruttschnitt Mineral Research Centre (JKMRC) developed two additional fragmentation models, the crush zone model (CZM) and the two-component model (TCM) (Djordjevic 1999; Kanchibotla et al. 1999; Thornton et al. 2001), to address the challenge of predicting the fine and course sections of the fragmentation curve.

As Kuz-Ram (Cunningham 2005) is the most widely used fragmentation formula, it is selected for use in this paper. The Kuz-Ram formula is given by

$$x_m = AK^{-4/5}Q^{1/6}\left(\frac{115}{R}\right)^{19/20}, \tag{9}$$

where x_m is the mean particle size (cm), A is the rock factor depending on the hardness and structure of the ground, K is the explosive powder factor (kg/m^3) and R is the weight strength of the explosive product relative to ammonium nitrate fuel oil.

The value of the rock factor, A, depends on different aspects of the ground including joints in geology, density and hardness. According to Ouchterlony (2003), using MWD data to determine A, such as in Raina et al. (2003), helps in monitoring blastability during an ongoing operation. In this paper, we assume that A is linearly proportional to hardness, η_{ij} ($A = \gamma\eta_{ij}$). This definition of A relies only on MWD data obtained from a network of automated drills (see Sect. 5 for future proposed work).

The objective of minimising the deviation in particle size (calculated using Eq. (9) for each hole) from the engineer-specified target particle size, $\hat{x}_m$, is given by

$$\min Z = \sum_{i=1}^{I}\sum_{j=1}^{J_i}\left[\hat{x}_m - \gamma\eta_{ij}\left(\frac{Q_{ij}}{d_{ij}\hat{B}_i\hat{S}_{ij}}\right)^{-4/5}Q_{ij}^{1/6}\left(\frac{115}{R_{ij}}\right)^{19/20}\right]^2. \tag{10}$$

2.4 Constraints

2.4.1 Energy Intensity

The selection of explosive product and, therefore, explosive energy intensity for a given hole is one of the decision variables. However, ground hardness constrains energy intensity, for three reasons.

First, high-energy explosive products have a high velocity of detonation (VOD). They require competent (hard) ground with sufficient confinement to enable full chemical reaction before the region around the hole breaks away (Johnson 2018). Incomplete reactions can result in poisonous nitrogen oxide fumes (NOx) and waste of explosives.

Second, increasing the explosive powder factor through significant increases in explosive intensity may result in a bimodal particle size distribution, with a large amount of fines produced around the "crush zone" of each hole and some large fragments elsewhere (Ouchterlony and Sanchidrián 2019). This is not ideal for iron ore operations, which aim to produce a consistent crushed lump product between 6.3 mm and 50 mm.

Third, there is more heave energy in lower-VOD products, which is the energy due to gasses expanding to displace rock fracture outwards. Although high VOD produces good results in massive rock formations with minimal joint cracking, for softer grounds, better blast performance is achieved through heave and through the movement of rock (Rock et al. 2005).

The energy intensity of the explosive product, ε, should not exceed the maximum intensity allowed by the hardness of the ground for that hole, $\varepsilon^{\max}$. The energy intensity is constrained by

$$\varepsilon_{ij} \leq \varepsilon_{ij}^{\max},\ i = 1, \ldots, I,\ j = 1, \ldots, J_i, \tag{11}$$

where $\varepsilon^{\max}$ is a discontinuous function of hardness, similar to the maximum energy concentration, E^0.

2.4.2 Ground Vibration

The most widely applied empirical equation (Nguyen et al. 2020) for predicting blast-induced peak particle velocity (PPV), and therefore ground vibration, is given by (Duvall and Petkof 1959)

$$PPV = \lambda \left(\frac{D}{\sqrt{W}} \right)^{\alpha}, \tag{12}$$

where PPV is the peak particle velocity (mm/s), λ, α are site factors that are determined using previous blasts, D is the distance to the sensitive site (m) and W is the maximum explosive charge weight per delay, which in the case of a single hole is equivalent to Q, the mass of the explosive in the hole (kg).

By rearranging Eq. (12) to solve for W (or Q), the maximum allowable mass of explosive product in a hole is constrained so that the sensitive site does not exceed the PPV limits.

$$\sqrt{Q_{ij}} \leq \frac{D_{ij}}{\sqrt[\alpha]{\frac{PPV}{\lambda}}},\ i = 1, \ldots, I,\ j = 1, \ldots, J_i, \tag{13}$$

where D_{ij} is the distance from the hole to the sensitive site (m).

2.4.3 Air Overpressure

A widely used formula (Nguyen and Bui 2019) for predicting air overpressure (AOp) (Kuzu et al. 2009) is

$$AOp = k \left(\frac{D}{\sqrt[3]{W}} \right)^{\beta}, \tag{14}$$

where AOp is air overpressure (dB), and k, β are site factors that are determined using previous blasts. The maximum allowable mass per hole to meet the AOp limits for a sensitive site is

$$\sqrt[3]{Q_{ij}} \leq \frac{D_{ij}}{\sqrt[\beta]{\frac{AOp}{k}}}, \; i = 1, \ldots, I, \; j = 1, \ldots, J_i. \tag{15}$$

2.4.4 Flyrock

Chiappetta et al. (1998) first introduced scaled depth of burial (SDoB) to limit flyrock from blasts during the widening of the Panama Canal so that rocks did not end up at the bottom of the canal. This widely used formula for limiting flyrock is given by

$$SDoB = \frac{Z_c}{\sqrt[3]{W_{10\phi}}}, \tag{16}$$

where $SDoB$ is the scaled depth of burial, the value of which depends on the distance of the hole from the sensitive site, ranging from 1.3 at close range to 1.0 at long range (m/$kg^{1/3}$), Z_c is the distance from the top of the hole to the centre of the crater charge ($Z_c = sl + 5\phi$, [m]) and $W_{10\phi}$ is the weight of the explosives in an explosive column of length equal to 10 hole diameters (kg).

Equation 16 uses the SDoB limit to determine the minimum stem length for a given hole depending on the hole's distance from the sensitive site and the explosive product intensity in the hole.

$$SDoB_{ij} \leq \frac{sl_{ij} + 5\phi}{\sqrt[3]{\pi(\frac{\phi}{2})^2 \rho_{ij} 10\phi}}, \; i = 1, \ldots, I, \; j = 1, \ldots, J_i, \tag{17}$$

where SDoB is a piecewise-constant function that depends on the distance from the sensitive site. McKenzie (2018) provides flyrock footprint plots with predicted maximum flyrock ranges of $\sim 230m$ for SDoB of $1.22m/kg^{1/3}$, $\sim 300m$ for SDoB of $1.11m/kg^{1/3}$ and $\sim 480m$ for SDoB of $0.89m/kg^{1/3}$. McKenzie (2018) includes a discussion on projection probabilities and appropriate factors of safety.

2.4.5 Other Constraints

The remaining constraints ensure that the design is achievable and realistic in practice. Equation (18) limits the spacing-to-burden ratio to the best-practice range to achieve good fragmentation (Singh et al. 2016). Equation (19) ensures that the rows of holes extend to the blast extents in the burden direction. Equation (20) ensures that holes in a row extend to blast extents in the spacing direction. Equations (21) and (22) ensure that the truck used for loading explosives can fit between the rows of holes so that an auger can be used to load holes (rather than inefficient and labour-intensive hose-loading). Finally, Eqs. (23) and (24) ensure that holes are deep enough to provide

adequate stemming and that the hole depth extends beyond the bench height (or top and bottom blast surfaces specified by the designer).

$$1 \leq \frac{\hat{S}_{ij}}{\hat{B}_i} \leq 1.4,\ i = 1, \ldots, I,\ j = 1, \ldots, J_i, \tag{18}$$

$$\sum_{i=1}^{I} \hat{B}_i + y_0 = y_{\max}, \tag{19}$$

$$\sum_{j=1}^{J_i} \hat{S}_{ij} + x_{i0} = x_i^{\max},\ i = 1, \ldots, I, \tag{20}$$

$$\hat{B}_i \geq \hat{B}_{\min},\ i = 1, \ldots, I, \tag{21}$$

$$\hat{S}_{ij} \geq \hat{S}_{\min},\ i = 1, \ldots, I,\ j = 1, \ldots, J_i, \tag{22}$$

$$d_{ij} \geq sl_{ij},\ i = 1, \ldots, I,\ j = 1, \ldots, J_i, \tag{23}$$

$$d_{ij} \geq d_{ij}^{\min},\ i = 1, \ldots, I,\ j = 1, \ldots, J_i. \tag{24}$$

Given all the input parameters, the above-described mathematical model can be used to determine optimal burden, spacing, hole dimensions, and explosive intensity in each hole for either the dig efficiency or the fragmentation objective. However, there are two challenges, as follows:

1. Modelling the input parameters: Some of the key parameters in the model are functions of the decision variables. For example, the hardness parameter is a function of hole position, as is the distance to the sensitive site.
2. Nonlinear integer problem: There are discrete variables such as the diameter of the hole and explosive product type. This means that the problem is a nonlinear discrete optimisation problem, and such problems are known to be computationally challenging to solve.

3 Methodology

We present a three-stage heuristic to determine the optimal burden, spacing, and explosive intensity in each hole for the entire pattern. In Stage 1, we determine the approximate position of each hole by a procedure called hole-by-hole optimisation (see Sect. 3.1). Using the approximate locations, ground hardness and limits (for energy intensity, vibration, flyrock and air overpressure) are estimated for each hole position as an input to Stage 2. This addresses the first challenge regarding input parameters as functions of the decision variables.

In Stage 2 (end-to-end optimisation described in Sect. 3.2), we solve the mathematical model for the entire blast pattern to determine exact hole positions. Stage 2 relaxes the diameter and explosive product variables to continuous values, with the optimal values rounded to the nearest discrete value. This addresses the second challenge regarding the discrete variables. In Stage 3, with hole positions, diameter, and explosive product types fixed as parameters (from the solution of Stage 2), we solve

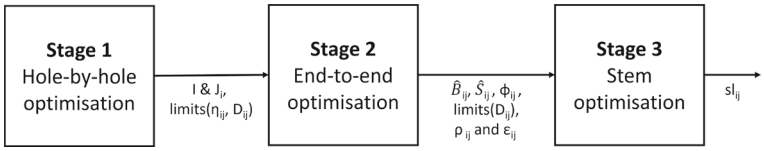

Fig. 6 Three-stage solution methodology for drill & blast design

the mathematical model to determine the optimal stem lengths and, hence, the mass of the explosive for each hole.

The three-stage methodology is depicted in Fig. 6. For each stage, the optimisation model to solve is a sub-model of the overall model in Sect. 2, formed by modifying the scope as required for that stage. For example, all stages use the same objective function, either Eq. (8) for dig efficiency or Eq. (10) for fragmentation. Additionally, each stage uses a subset (as applicable) of the constraints defined by Eqs. (11), (13), (15), (17) and (18) to (24). This is described in detail in the following sections. The sub-model in each stage can be solved in Python using Ipopt, the interior point optimizer.

3.1 Hole-by-Hole Optimisation

The aim of this stage is to determine the approximate locations for each hole by dividing the entire blast pattern into small segments such that each segment contains only one hole. To achieve this, we first determine the optimal burden by progressing from the open face to the opposite blast boundary in the y-axis as shown in Fig. 7. The following are the steps to determine the optimal burden:

Step 1. As illustrated in Fig. 7, select a region between $y = y_0$ and a predefined maximum possible burden, $B_{\max}$, from the open face. To solve the mathematical model for one row, divide the row into sub-regions (each of width $S_{\max}$). Each sub-region has area $B_{\max} \times S_{\max}$. Estimate the MWD hardness, $\eta(x)$ (Eq. (1)), at the centre of each sub-region using the discrete hardness values, η_p, and the weighted inverse distance squared, ω_p, with respect to the centroid of the sub-region. Use the hardness value for each sub-region to calculate the limits for maximum energy intensity (Eq. (11)). Use the distance from the centroid of the sub-region to the sensitive site to calculate the limits for vibration (Eq. (13)), air overpressure (Eq. (15)), and flyrock (Eq. (17)).

Step 2. The whole region defined in step 1 is treated as a single hole in this step. From the constraint limits from the sub-regions in step 1, take the lowest limits for vibration and air overpressure, the highest limit for flyrock (SDoB) and the average hardness over the sub-regions as the input. Depending on the objective, use Eq. (8) for dig efficiency or use Eq. (10) for fragmentation to determine the optimal burden, y_1, and spacing for a single hole with hardness and constraint limits as defined above. Discard spacing and create a new region between y_1 and $y_1 + B_{\max}$.

Step 3. Using the same process as above, calculate the optimal burden, y_2, for the new region.

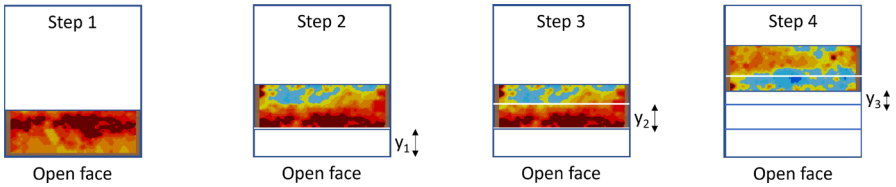

Fig. 7 Creation of regions for optimal burden calculation (blue hard, red soft material)

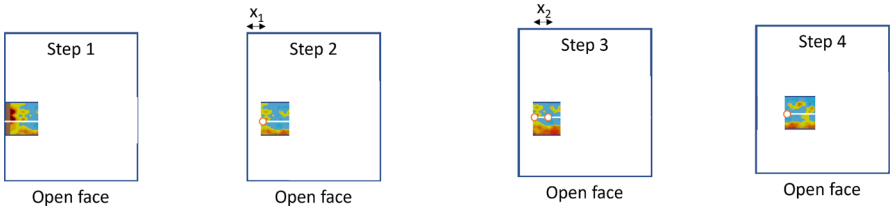

Fig. 8 Creation of regions for optimal spacing calculation (blue hard, red soft material)

Step 4. Move the region of interest and repeat the above steps for the remainder of the blast area.

After calculating the optimal burden for each row according to the above procedure, we calculate the optimal spacing within each row as shown in Fig. 8. This process is detailed in the following steps:

Step 1. As illustrated in Fig. 8, for a given row, i, select a region bounded between x_{i0} and $S_{\max}$ from the left of the pattern and by $1/2B_i$ from either side of the row.

Step 2. Using the same methodology as for burden, calculate the hardness, $\eta(x)$, and constraints for the centroid of the region. Using B_i, $\eta(x)$, limits and depending on the objective, by using Eq. (8) for dig efficiency or Eq. (10) for fragmentation, determine the optimal spacing, x_1. Move the hardness region to x_1 to $x_1 + S_{\max}$.

Step 3. Using the same process as above, calculate the optimal spacing for the new region, x_2.

Step 4. Move the region of interest and repeat the above steps for the rest of the row.

Hole-by-hole optimisation provides the number of rows in the pattern and the number of holes in each row. Although the procedure calculates all of the decision variables, including diameter, hole positions, and explosive product intensity, only the number of rows and number of holes in each row, hardness of each hole and limits are sent to the next stage. During the above calculations, we increase the horizontal extents of the pattern. The reason for this is explained below.

3.2 End-to-End Optimisation

The end-to-end optimiser uses I and J_i to optimise hole positions by allowing them to flex subject to the fixed hardness values and constraint limits defined in Stage 1. This enables the hardness parameter to be independent of hole location and, in turn, allows optimisation of the full blast area.

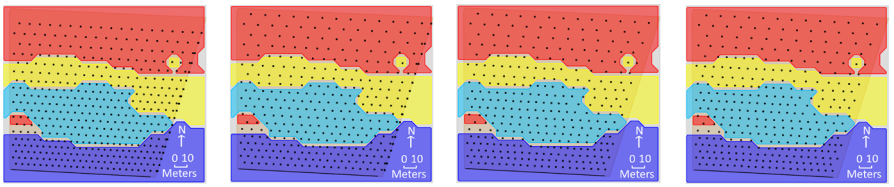

Fig. 9 Output of each optimisation stage—from left to right: hole-by-hole, first iteration end-to-end, second iteration end-to-end and stem optimisation (blue hard, red soft material)

End-to-end optimisation determines the decision variables through two iterations of complete pattern optimisation based on minimising the overall objective value (either dig efficiency or fragmentation) summed over all holes. In the first iteration, we use I and J_i from the hole-by-hole stage and optimise all variables. After the first iteration, some of the hole locations can occur outside of the blast extents since the extent constraint is relaxed in this iteration.

In the second iteration, we round the diameter and explosive energy to the nearest allowed value and fix them in place, then impose the extent constraint, and again optimise all other variables. This is because there are only a discrete number of drill bits, and explosive products are limited to the explosive recipe configurations available in the mobile processing unit. Therefore, continuous diameter and explosive product energy values from the first iteration are rounded to the nearest available value and fed as input parameters to the second iteration.

Sub-optimality is introduced as a result of rounding. As an alternative solution approach, it would be possible to repeat the optimisation separately for each available diameter at the site. In fact, for the case studies in Sect. 4, the historical design diameter is used as the input parameter. Since there is only one global diameter variable, it is computationally tractable to solve the optimisation for each possible diameter. There are far more explosive product variables (one for each hole), and hence this approach would not be possible for these variables. End-to-end optimisation determines the positions of holes and all other decision variables, except for stem heights, and feeds these to the final stage.

3.3 Stem Optimisation

The purpose of stem optimisation is to ensure that the changes to hole positions produced by end-to-end optimisation do not violate the constraints. Stem optimisation imposes the air overpressure, flyrock and ground vibration constraints by adjusting the stem height. All previous decision variables, except for stem height, are used as input parameters to solve for the stem height of each hole. This ensures that the mass of the product for each hole is adjusted to comply with air overpressure and ground vibration constraints, and the stem height for each hole is adjusted to comply with flyrock constraints.

Figure 9 shows the output of each stage for a simulation using the fragmentation objective. Extra holes are visible at the right boundary of the blast for the hole-by-hole

and the first iteration of the end-to-end optimisation as clusters of holes bunched up together.

4 Results and Discussion

To validate the methodology, we use 10 historical blast patterns from a Rio Tinto-operated mine site. We use the two objectives from Sect. 2, dig efficiency and fragmentation, and compare the objective values for our approach with that of existing designs (original designs). To obtain the objective value for an original design, we fix the burden and spacing to that of the existing design and solve the model for only stem length and explosive product. Our methodology can also be used to optimise constant burden and spacing. Hence, we also present a comparison between variable versus constant burden and spacing designs. For all the experiments, we set the diameter to 0.23 m, which is used in the original design. For the rest of the section, "O" refers to the original designs, "C" refers to optimised constant burden and spacing, and "V" refers to variable burden and spacing.

Table 1 presents the results for the dig efficiency objective. Dig efficiency is calculated for each hole, and the average and standard deviation (SD) over all holes are reported in the table. For example, for Blast 1, mean and standard deviation values for the original, optimised constant and variable designs are calculated using 445, 539, and 490 holes, respectively. The "diff %" is the difference between variable optimised (V) and constant optimised (C) designs. Using our approach, both the constant and the variable optimised designs can improve dig efficiency from an average of 80% (average over all original designs) to more than 95%. Over all the blasts, the dig efficiency is ∼2% better if we use variable design compared to constant design, while using ∼11% fewer holes.

Table 2 presents the results for the fragmentation objective with a target particle size of 30 cm. As above, the mean and standard deviation are reported over all holes. The effect of variable design is more pronounced on fragmentation than on dig deficiency, with the variable design achieving between 3% and 23% better adherence to the target mean particle size than with constant design. The standard deviation is also smaller for most of the variable designs (all blasts except for one) with an overall 5% lower standard deviation than the constant design. Here too, variable designs achieve better results overall, ∼9% closer to target size, using ∼13% fewer holes than constant design.

The reduced standard deviation from the target particle size for variable designs is important, as crushers have an optimal feed size range. For iron ore, over-blasting results in a higher percentage of material under the lump product size threshold (∼7 mm). A blast with a significant standard deviation from the target could also create oversize rocks. This impacts productivity as it requires activation of specialised rock-breaking machinery (either at the crusher or the oversize stockpile) or secondary blasting (side casting of large rocks and drill and blasting at next blast).

While the focus of this paper is on pattern design, it is important to remember that charge design is also a decision variable in the problem. For example, in constant burden and spacing, the same model can be used to optimise charge designs through the explosive amounts and stem lengths. This ensures that the amount of explosives

Table 1 Outcome of case studies using dig efficiency as the objective function

Blast	Number of holes				Mean dig efficiency				SD dig efficiency		
	O	C	V	diff %	O[2]	C	V	diff %	C	V	diff %
1	445	539	490	−9	0.86	0.96	0.96	0	0.05	0.02	−3
2	661[1]	819	742	−9	0.77	0.94	0.97	3	0.03	0.03	0
3	672	879	793	−10	0.84	0.93	0.99	6	0.05	0.04	−1
4	293	258	234	−9	0.91	0.89	0.98	9	0.05	0.04	−1
5	426[1]	793	689	−13	0.88	0.95	0.99	4	0.05	0.04	−1
6	801	892	792	−11	0.87	0.97	0.96	−1	0.03	0.04	1
7	667[1]	1,120	1,004	−10	0.65	0.97	0.98	1	0.04	0.04	0
8	717	813	776	−5	0.74	0.94	0.96	2	0.06	0.06	0
9	933[1]	950	817	−14	0.76	0.96	0.97	1	0.04	0.04	0
10	909	1,312	1,112	−15	0.65	0.95	0.96	1	0.04	0.03	−1
All		**8,375**	**7,449**	**−11**	**0.80**	**0.95**	**0.97**	**2**	**0.05**	**0.04**	**−1**

Dig efficiency is the blast effect to dig efficiency contribution expressed in decimals. The diff % column represents the percentage difference between constant (C) and variable (V) designs

[1]The original pattern (O) does not contain holes for the entire extent of the blast. For these blasts, it is only meaningful to compare the optimised constant versus optimised variable design and not the original.

[2]Simulated by fixing the burden and spacing to the original design and then solving the model for only stem length and explosive product

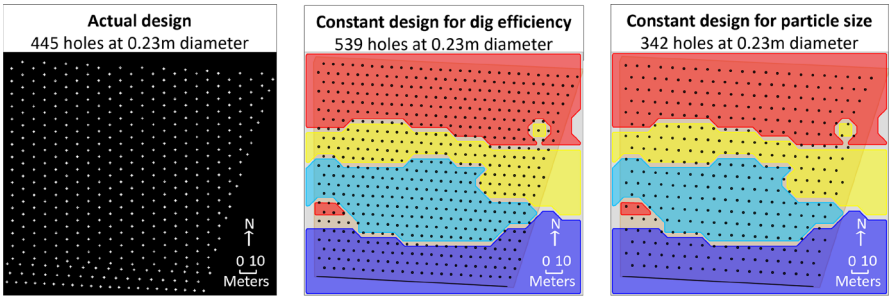

(a) Optimised constant design – blue hard, red soft material

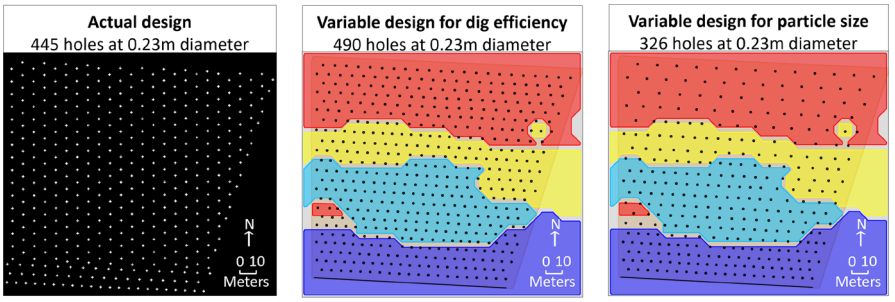

(b) Optimised variable design – blue hard, red soft material

Fig. 10 Blast 1 Design Options

Table 2 Outcome of case studies using fragmentation as the objective function

Blast	Number of holes				Mean size deviation				SD size deviation		
	O	C	V	diff %	O^2 cm	C cm	V cm	diff %	C cm	V cm	diff %
1	445	342	326	−5	11.34	10.20	3.27	−23	5.69	3.34	−8
2	661[1]	512	419	−18	7.94	4.78	4.01	−3	6.41	4.24	−7
3	672	553	461	−17	11.50	8.63	5.33	−11	7.07	4.73	−8
4	293	144	126	−13	11.76	5.18	3.58	−5	4.62	3.95	−2
5	426[1]	534	433	−19	5.75	4.90	3.43	−5	4.42	4.86	1
6	801	569	484	−15	10.35	7.18	3.16	−13	6.06	3.81	−8
7	667[1]	729	679	−7	5.48	5.72	2.58	−10	4.70	3.84	−3
8	717	636	547	−14	8.15	6.85	3.17	−12	5.65	4.11	−5
9	933[1]	506	425	−16	7.14	7.93	5.00	−10	5.59	4.84	−3
10	909	745	664	−11	3.75	2.97	2.01	−3	4.29	3.44	−3
All		**5,270**	**4,564**	**−13**	**8.32**	**6.24**	**3.42**	**−9**	**5.86**	**4.25**	**−5**

Mean size deviation is the deviation of the resulting particle size from target particle size in centimetres (cm). The diff % column represents the percentage difference between constant (C) and variable (V) designs with respect to 30 cm target size. For example, a 3 cm difference is 10%.

[1]The original pattern (O) does not contain holes for the entire extent of the blast.

[2] Simulated by fixing the burden and spacing to the original design and then solving the model for only stem length and explosive product

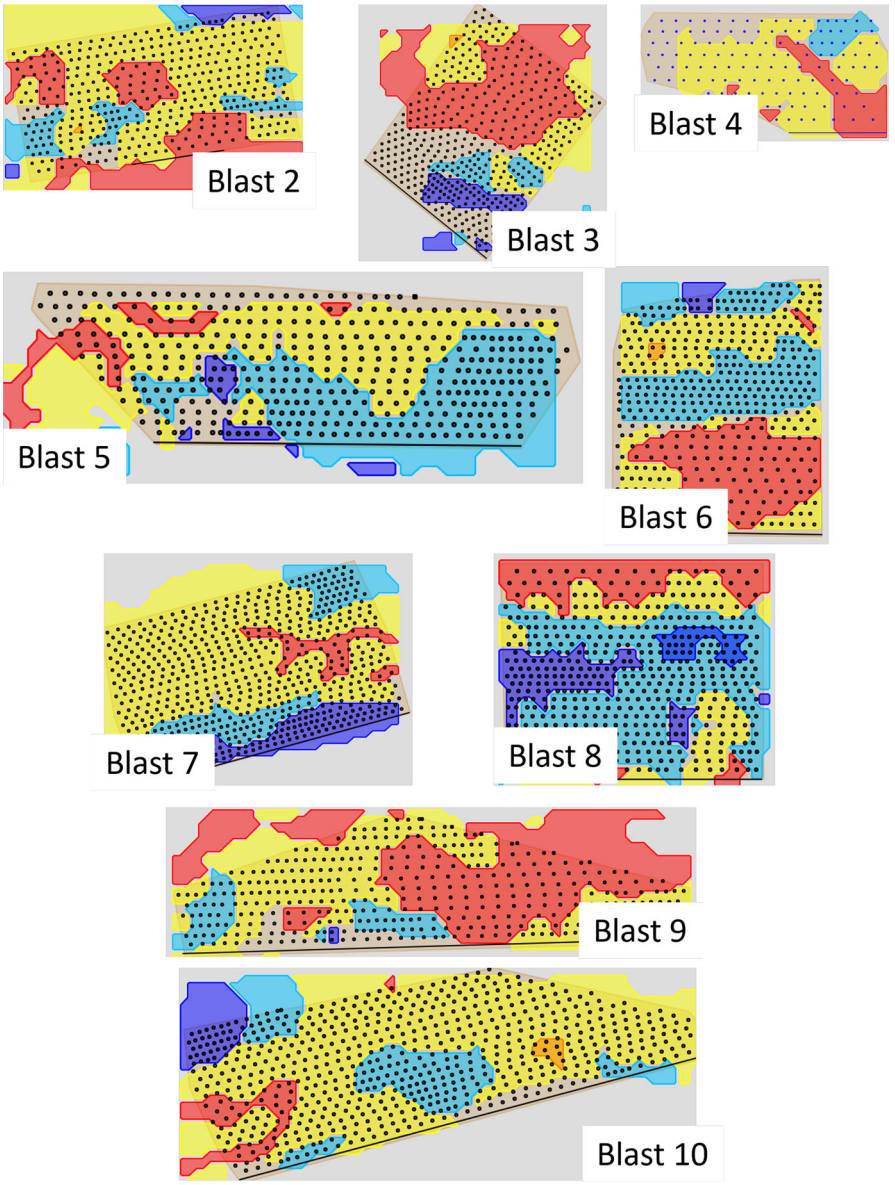

Fig. 11 Variable designs with fragmentation objective. Red is soft, yellow is medium, light blue is hard, dark blue is extra hard and tan is unknown (treated as medium)

can be adjusted in conjunction with the hole position. This is important for setting initiation delays for timing design because it alleviates the risk of exceeding constraints during timing due to the type or amount of explosives. Future work will verify this simplification step to timing design.

Figure 10a and b show a top-down view of historical, variable and constant designs for Blast 1. For the optimised constant design, optimisation for dig efficiency uses more

holes than the original design. However, optimisation for particle size uses fewer holes. The variable design uses fewer holes for both types of optimisation. Notwithstanding the reduced hole count, the variable design achieves similar dig efficiency and significantly better adherence to the particle size target than the optimised constant design (refer to Tables 1 and 2 for details).

Variable designs have more scope to improve outcomes in complex geology, with significant improvements to fragmentation. For example, the ground hardness for Blast 1 (see Fig. 10b) is highly variable compared to Blast 2 (see Fig. 11). The improvement in fragmentation from constant to variable design is 23% for Blast 1 and 3% for Blast 2. Figure 11 demonstrates the variability in pattern design outcomes for Blasts 2 to 10.

5 Conclusion

This paper presents a heuristic approach to D&B design to meet fragmentation or dig efficiency objectives, using MWD data from a network of drills to enable high-resolution estimates of ground hardness. We showed that variable designs can better exploit this information to accommodate for variances in hardness to achieve blast objectives with fewer holes.

Our methodology resolves two key challenges to variable designs. The first challenge is estimating the precise values of input parameters, given that they are functions of the decision variables. Our approach was to divide the blast into small regions with one hole per region and to iteratively determine the optimal position within this region, allowing the respective inputs to be fixed at the value for this position. The second challenge is solving a nonlinear discrete optimisation problem with discrete variables such as the diameter of the holes. We addressed this by first relaxing the discrete constraints to continuous and then fixing the values of the discrete variables to the closest rounded values.

Delivering blast objectives involves a trade-off between operational complexity (or cost) versus fragmentation and diggability. The results show that better fragmentation and diggability outcomes can often be achieved through variable designs. However, this comes at an increased operational complexity, as it is more challenging to execute a design with varying burden and spacing across the blast. A weakness of the current optimisation approach is that it does not optimise for complexity or cost.

Future models will incorporate operational complexity and cost to achieve an operational optimum and will consider the total cost of mine operation (from extraction to crushing). However, the novelty and potential of the research in this paper is the variable designs. Simulation outcomes suggest that variable designs not only achieve better fragmentation and diggability, but also reduce the number of holes and therefore the cost (compared to fixed designs).

The optimisation tool that was built as an outcome of this research provides decision assistance to engineers by analysing many scenarios quickly. Each scenario takes $\sim$1 min to run (on a Laptop with 32 GB RAM and i7-10850 H 2.7GHz CPU) and can be processed in parallel in the future to provide many design options. The selected option is easily exportable to standard D&B design tools to make subtle refinements,

perform timing design and for additional simulation. The importance of such tools is demonstrated by Bakhtavar et al. (2022), where outcomes of over 100 blasts were analysed to model adverse effects such as vibration on the environment and infrastructure. This tool can help support this type of analysis through rapid generation and comparison of different design scenarios.

The next phase of research will focus on validating optimisation outputs and calibrating MWD hardness to rock factor conversion through field trials. We will also investigate anisotropy and other techniques to improve hardness estimation. Note, however, that there will always be limits even with more advanced estimation techniques, since the ground structure, such as joint spacing, is not extrapolated from MWD algorithms.

Future models will also explore the multi-objective optimisation problems, including an objective to reduce pollutants such as that in Abdollahisharif et al. (2016). These could use a single combined objective function with weights attached to each objective. However, the challenge is in selecting the weights appropriately, as the different objectives are typically in different units.

Funding Open Access funding enabled and organized by CAUL and its Member Institutions This work is funded by Rio Tinto.

Data Availability Not applicable.

Declarations

Conflict of interest The authors Ozan Perincek and Daniel Arthur are employed by Rio Tinto.

References

Abdollahisharif J, Bakhtavar E, Nourizadeh H (2016) Monitoring and assessment of pollutants resulting from bench-blasting operations. J Min Environ 7(3):109–118

Aryafar A, Rahimdel J, Tavakkoli E (2020) Selection of the most proper drilling and blasting pattern by using madm methods (a case study: Sangan iron ore mine, iran). Rudarsko-geološko-naftni zbornik 35(3):97–108

Bakhtavar E, Abdollahisharif J, Ahmadi M (2017) Reduction of the undesirable bench-blasting consequences with emphasis on ground vibration using a developed multi-objective stochastic programming. Int J Min Reclam Environ 31(5):333–345

Bakhtavar E, Sadiq R, Hewage K (2021) Optimization of blasting-associated costs in surface mines using risk-based probabilistic integer programming and firefly algorithm. Nat Resour Res 30(6):4789–4806

Bakhtavar E, Abdollahisharif J, Mohammadi D (2022) Analysis and improvement of blasting operation in porphyry, diorite dyke, and trachyte sungun zones: In-situ investigations. Int J Min Geo-Eng 56(1):19–24

Chiappetta RF, Treleaven T, Nixon E, Smith JD (1998) History and expansion of the panama canal. Fragblast 2(3):313–340
Cunningham CVB (1987) Fragmentation estimations and kuz-ram model-four years on. In: Proceedings of the 2nd International Symposium on Rock Fragmentation by Blasting, pp 475-487
Cunningham CVB (2005) The kuz-ram fragmentation model–20 years on. In: Brighton conference proceedings of 3rd World Conference on Explosives and Blasting, Vol 4, pp 201–210
Djordjevic N (1999) Two-component model of blast fragmentation, In: Proceedings of 6th International Symposium for Rock Fragmentation by Blasting, Symposium Series S21
Duvall WI, Petkof B (1959) Spherical Propagation of Explosion-generated Strain Pulses in Rock. U.S, Department of the Interior, Bureau of Mines
Ebrahimi E, Monjezi M, Khalesi MR, Armaghani DJ (2016) Prediction and optimization of back-break and rock fragmentation using an artificial neural network and a bee colony algorithm. Bull Eng Geol Environ 75(1):27–36
Enayatollahi I, Aghajani Bazzazi A, Asadi A (2014) Comparison between neural networks and multiple regression analysis to predict rock fragmentation in open-pit mines. Rock Mech Rock Eng 47(2):799–807
Esmaeili M, Salimi A, Drebenstedt C, Abbaszadeh M, Aghajani Bazzazi A (2015) Application of PCA, SVR, and ANFIS for modeling of rock fragmentation. Arab J Geosci 8(9):6881–6893
Fang Q, Nguyen H, Bui XN, Nguyen-Thoi T, Zhou J (2021) Modeling of rock fragmentation by firefly optimization algorithm and boosted generalized additive model. Neural Comput Appl 33(8):3503–3519
Hasanipanah M, Amnieh HB, Arab H, Zamzam MS (2018) Feasibility of PSO-ANFIS model to estimate rock fragmentation produced by mine blasting. Neural Comput Appl 30(4):1015–1024
Haugg C, Perincek O, McNeilage C (2023) The use of machines as sensors to optimise drill and blast outcomes. In: 26th World Mining Congress proceedings, Brisbane
Hosseini S, Monjezi M, Bakhtavar E (2022) Minimization of blast-induced dust emission using gene-expression programming and grasshopper optimization algorithm: a smart mining solution based on blasting plan optimization. Clean Technol Environ Policy 24(8):2313–2328
Jia Z, Song Z, Fan J, Jiang J (2022) Prediction of blasting fragmentation based on GWO-ELM. Shock Vib 2022:1–8
Johnson C (2018) Effect of wave collision on fragmentation, throw, and energy efficiency of mining and comminution. In: Awuah-Offei K (ed) Energy Efficiency in the Minerals Industry: Best Practices and Research Directions. Springer International Publishing, Cham, pp 55–70
Kanchibotla S, Valery W, Morrell S (1999) Modelling fines in blast fragmentation and its impact on crushing and grinding. Explo '99-A Conf on 99:137–144
Khoshrou H, Badroddin M, Bakhtavar E (2010) Determination of the practicable burden in sungun open-pit mine, Iran. In: Proceedings of the 9th International Symposium on Rock fragmentation by blasting., Taylor & Francis Group
Kuzu C, Fisne A, Ercelebi SG (2009) Operational and geological parameters in the assessing blast induced airblast-overpressure in quarries. Appl Acoust 70(3):404–411
Lu GY, Wong DW (2008) An adaptive inverse-distance weighting spatial interpolation technique. Comput Geosci 34(9):1044–1055
McKenzie C (2018) Flyrock model validation. In: International Society of Explosives Engineers, 4th Annual Conferance, Fremantle proceedings
Mokhtari A, Monjezi M (2015) Application of multi-criteria decision making models in designing blasting pattern of gole-e-gohar (mine # 1) iron mine. Iran J Min Eng 9(25):35–43
Monjezi M, Amiri H, Farrokhi A, Goshtasbi K (2010) Prediction of rock fragmentation due to blasting in sarcheshmeh copper mine using artificial neural networks. Geotech Geol Eng 28(4):423–430
Monjezi M, Bahrami A, Yazdian Varjani A (2010) Simultaneous prediction of fragmentation and flyrock in blasting operation using artificial neural networks. Int J Rock Mech Min Sci (1997) 47(3):476–480
Nguyen H, Bui XN (2019) Predicting blast-induced air overpressure: a robust artificial intelligence system based on artificial neural networks and random forest. Nat Resour Res 28(3):893–907
Nguyen H, Drebenstedt C, Bui XN, Bui DT (2020) Prediction of blast-induced ground vibration in an open-pit mine by a novel hybrid model based on clustering and artificial neural network. Nat Resour Res 29(2):691–709
Ouchterlony F (2003) Influence of blasting on the size distribution and properties of muckpile fragments: a state-of-the-art review. Technical report

Ouchterlony F (2005) The swebrecfunction: linking fragmentation by blasting and crushing. Inst Mining Metall Trans Sect A Mining Technol 114(1):29–44
Ouchterlony F, Sanchidrián JA (2019) A review of development of better prediction equations for blast fragmentation. J Rock Mech Geotech Eng 11(5):1094–1109
Perincek O, Williams R, Haugg C, Thomas M, Beswick M (2024) Method for improved drilling and blasting in open cut mines. International Patent WO2024077346
Raina AK, Ramulu M, Choudhury PB, Dudhankar A, Chakraborty AK (2003) Fragmentation prediction in different rock masses characterised by drilling index. In: Proceedings of the seventh international symposium on rock fragmentation by blasting, Beijing 7:117–121
Rock J, Maurer A, Pereira N (2005) Coming of age for low-density explosives. In University of Wollongong and the Australasian Institute of Mining and Metallurgy (ed Aziz, N), editor, Coal Operators' Conference, Proceedings of the 2005 Coal Operators' Conference, ro.uow.edu.au, 175-182
Salmi EF, Sellers EJ (2021) A review of the methods to incorporate the geological and geotechnical characteristics of rock masses in blastability assessments for selective blast design. Eng Geol 281:105970
Segarra P, Sanchidrián JA, López LM, Querol E (2010) On the prediction of mucking rates in metal ore blasting. J Min Sci 46(2):167–176
Singh PK, Roy MP, Paswan RK, Sarim KS, Ranjan Jha R (2016) Rock fragmentation control in opencast blasting. J Rock Mech Geotech Eng 8(2):225–237
Thornton D, Kanchibotla S, Esterle J (2001) A fragmentation model to estimate rom size distribution of soft rock types. In: Proceedings of the 27th Annual Conference on Explosives and Blasting Technique, Vol 1, pp 41–53
Yari M, Bagherpour R, Jamali S, Asadi F (2015) Selection of most proper blasting pattern in mines using linear assignment method: sungun copper mine. Arch Min Sci. https://doi.org/10.1515/amsc-2015-0025
Zhou J, Li C, Arslan CA, Hasanipanah M, Bakhshandeh Amnieh H (2021) Performance evaluation of hybrid FFA-ANFIS and GA-ANFIS models to predict particle size distribution of a muck-pile after blasting. Eng Comput 37(1):265–274
Zhou J, Zhang Y, Qiu Y (2024) State-of-the-art review of machine learning and optimization algorithms applications in environmental effects of blasting. Artif Intell Rev 57(1):5